CT&F Ciencia, Tecnología y Futuro
ISSN: 0122-5383
ctyf@ecopetrol.com.co
ECOPETROL S.A.
Colombia

Escobar, Freddy-Humberto; Martinez, Javier-Andrés; Montealegre-Madero, Matilde
Conventional pressure analysis for naturally fractured reservoirs with transition period before and after the radial flow regime
CT&F Ciencia, Tecnología y Futuro, vol. 3, núm. 5, diciembre, 2009, pp. 85-106
ECOPETROL S.A.
Bucaramanga, Colombia

CT&F
Ciencia, Tecnología y Futuro

CONVENTIONAL PRESSURE ANALYSIS FOR NATURALLY FRACTURED RESERVOIRS WITH TRANSITION PERIOD BEFORE AND AFTER THE RADIAL FLOW REGIME

Freddy-Humberto Escobar[1*], Javier-Andrés Martinez[2] and Matilde Montealegre-Madero[3]

[1,2,3] Universidad Surcolombiana, Neiva, Huila, Colombia

e-mail: fescobar@usco.edu.co e-mail: j_martinez70@hotmail.com e-mail: matildemm@hotmail.com

(Received April 30, 2008; Accepted October 5, 2009)

It is expected for naturally occurring formations that the transition period of flow from fissures to matrix takes place during the radial flow regime. However, depending upon the value of the interporosity flow parameter, this transition period can show up before or after the radial flow regime. First, in a heterogeneous formation which has been subjected to a hydraulic fracturing treatment, the transition period can interrupt either the bilinear or linear flow regime. Once the fluid inside the hydraulic fracture has been depleted, the natural fracture network will provide the necessary flux to the hydraulic fracture. Second, in an elongated formation, for interporosity flow parameters approximated lower than $1x10^{-6}$, the transition period takes place during the formation linear flow period. It is desirable, not only to appropriately identify these types of systems but also to complement the conventional analysis with the adequate expressions, to characterize such formations for a more comprehensive reservoir/well management.

So far, the conventional methodology does not account for the equations for interpretation of pressure tests under the above two mentioned conditions. Currently, an interpretation study can only be achieved by non-linear regression analysis (simulation) which is obviously related to non-unique solutions especially when estimating reservoir limits and the naturally fractured parameters. Therefore, in this paper, we provide and verify the necessary mathematical expressions for interpretation of a vertical well test in both a hydraulically-fractured naturally fractured formation or an elongated closed heterogeneous reservoir. The equations presented in this paper could provide good initial guesses for the parameters to be used in a general nonlinear regression analysis procedure so that the non-uniqueness problem associated with nonlinear regression may be improved.

Keywords: *Dual-linear flow regime, radial flow regime, interporosity flow parameter, dimensionless storativity ratio*

* *To whom correspondence may be addressed*

Se espera en formaciones naturalmente fracturadas que el periodo de transición de las fisuras a la matriz tome lugar durante el flujo radial. Sin embargo, dependiendo del valor del parámetro de flujo interporoso, esta transición puede ocurrir antes o después del flujo radial. El primer caso, en una formación heterogénea que ha sido sometida a un tratamiento de fracturamiento hidráulico, la transición puede interrumpir el flujo bilineal o lineal tempranos. Una vez existe depleción de flujo en la fractura hidráulica, éste es restablecido por flujo procedente de la red de fracturas naturales. En el segundo escenario, en una formación alargada, para parámetros de flujo aproximadamente menores a $1x10^{-6}$, el periodo de transición ocurre durante el flujo lineal en la formación. Se desea no solo identificar estos sistemas apropiadamente sino complementar la técnica convencional con las expresiones adecuadas para caracterizar tales formaciones de modo que se tenga un manejo más comprensivo del yacimiento/pozo.

Hasta ahora, la técnica convencional no cuenta con las ecuaciones para interpretar pruebas de presión bajo las dos condiciones arriba descritas. Actualmente, la única forma de interpretación se conduce mediante técnicas de regresión no lineal (simulación) lo que conlleva a problemas de múltiples respuestas especialmente cuando se estiman los límites del yacimiento y los parámetros del yacimiento naturalmente fracturado. Por tanto, en este artículo, se proporcionan y verifican las expresiones matemáticas necesarias para interpretar pruebas de presión en un pozo vertical tanto en sistemas naturalmente fracturados interceptados por una fractura hidráulica, como en formaciones heterogéneas alargadas. Las ecuaciones presentadas en este artículo podrían proporcionar valores iniciales más representativos de los parámetros usados en un procedimiento general de regresión no lineal, de modo que se puedan reducir los problemas de multiplicidad de soluciones asociadas con este método.

Palabras Clave: *Régimen de flujo dual lineal, régimen flujo radial, parámetro de flujo interporoso, coeficiente de almacenaje adimensionales*

NOMENCLATURE

4n(n+2)12 = Slab model, 32 = Matchstick model, 60 cubic model

A	Area, (ft2)
B	Oil formation factor, (rb/STB)
C_{fD}	Dimensionless fracture conductivity
c_t	Compressibility, (1/psi)
h	Formation thickness, (ft)
h_m	Matrix block height, (ft)
k_f	Fracture bulk permeability, (md)
k_{fb}	Matrix permeability, (md)
$k_f w_f$	Fracture conductivity, (md-ft)
m	Slope
P	Pressure, (psi)
P_D	Dimensionless pressure
P_i	Initial reservoir pressure, (psi)
P_{wf}	Well flowing pressure, (psi)
P_{ws}	Well static pressure, (psi)
q	Flow rate, (bbl/D)
r_w	Well radius, (ft)
s_{DL}	Geometric skin factor due to the convergence of radial to dual-linear flow
s_L	Geometric skin factor due to the convergence of dual-linear to single-linear flow
s_r	Mechanical skin factor
T	Time, (hr)
t_D	Dimensionless time
t_{DA}	Dimensionless time based on reservoir area
t_{Dxf}	Dimensionless time based on half-fracture length
t_{max}	Time corresponding to the maximum pressure derivative of the transition period during either bilinear or linear flow regime, (hr)
t_{min}	Time corresponding to the minimum pressure derivative of the transition period, (hr)
x_f	Half-fracture length, (ft)
Y_E	Reservoir width, (ft)
W_D	Dimensionless reservoir width, (ft)

GREEK

Δ	Change, drop
Δt	Flow time, (hr)
ΔP_{1hr}	Pressure drop read at t = 1 hr, (psi)
$\emptyset$	Porosity, fraction
μ	Viscosity, (cp)
λ	Interporosity flow parameter between matrix and fissures
λf	Interporosity flow parameter between hydraulic fracture and fissures
ω	Dimensionless storativity (capacity) ratio

SUFFICES

BL	Bilinear flow
D	Dimensionless
DA	Dimensionless referred to reservoir area
DLF	Dual-linear flow
f	Fracture network, fissures
f+*m*	Total system (fracture network + matrix)
i	Initial conditions
L	Single-linear flow
LF	Single-linear flow
m	Matrix, slope
max	Maximum
min	Minimum

INTRODUCTION

Recently, Tiab and Bettam (2007) have introduced a technique to interpret pressure and pressure derivative tests in heterogeneous formations drained by a hydraulically fractured vertical well. Also, we are aware that an important number of pressure tests are conducted in long and narrow reservoirs which may possess heterogeneous nature with very low mass transfer capacity between fracture network and matrix. In the first case, the transition period may take place before the radial flow is developed. Once the flux in the hydraulic fractured is depleted, the naturally occurring fractures fed the hydraulic fracture, allowing the development of the transition period. In the second case, the phenomenon occurs after radial flow is vanished. During either dual-linear or linear flow regime in the formation, the fracture network fluid is depleted and, then, being reestablished from the matrix, leads to the presence of the transition period. In both cases, this transition period takes a "V" shape on the pressure derivative curve.

Among the investigations on pressure tests for elongated systems during this decade, Escobar *et al.* (2007a) introduced the application of the *TDS* technique for characterization of long and homogeneous reservoirs presenting new equations for estimation of reservoir area, reservoir width and geometric skin factors. Characterization of pressure tests in elongated systems using the conventional method was presented by Escobar and Montealegre (2007). Also, Escobar *et al.* (2007b) provided a way to estimate reservoir anisotropy when reservoir width is known in the mentioned systems from the combination of information obtained from the linear and radial flow regimes.

In this work, new expressions to complement the conventional technique are presented for interpretation of pressure tests in naturally occurring formations when the transition period takes place either before of after the radial flow regime. The proposed equations were verified with several examples.

MATHEMATICAL MODEL

The main assumptions considered in this work are: a slightly compressible and constant viscosity fluid flows throughout a constant thickness reservoir with constant matrix and fracture permeability and porosity, the well fully penetrates the producing formation. Flow from the natural fracture network to either hydraulic fracture or matrix occurs under pseudosteady state conditions. Neither wellbore storage nor geomechanical skin factor nor gravity effects are considered.

The dimensionless quantities are defined as:

$$P_D = \frac{k_{fb} h \Delta P}{141{,}2 \mu B} \qquad (1.1)$$

$$t_D = \frac{0{,}0002367\, k_{fb} t}{\mu (\phi c_t)_{f+m} r_w^2} \qquad (1.2.a)$$

$$t_{DA} = \frac{0{,}0002367\, k_{fb} t}{\mu (\phi c_t)_{f+m} A} \qquad (1.2.b)$$

$$t_{Dxf} = \frac{0{,}0002367\, k_{fb} t}{\mu (\phi c_t)_{f+m} x_f^2} \qquad (1.2.c)$$

$$C_{fb} = \frac{k_f w_f}{k_{fb} x_f} \qquad (1.3)$$

$$W_D = \frac{Y_E}{r_w} \qquad (1.4)$$

The naturally fractured reservoir parameters, dimensionless storativity (capacity) ratio and interporosity flow, introduced by Warren and Root (1963) were defined by:

$$\omega = \frac{\phi_f c_f}{\phi_f c_f + \phi_m c_m} \qquad (1.5)$$

$$\lambda = \frac{4n(n+2) k_m r_m^2}{4 k_{fb} h_m^2} \qquad (1.6)$$

THE TRANSITION PERIOD OCCURS BEFORE RADIAL FLOW REGIME

According to Tiab and Bettam (2007) the bilinear flow regime of a finite-conductivity hydraulic fracture in a heterogeneous formation is governed by:

$$P_D = \frac{2{,}451}{\sqrt{C_{fD}}}\left(\frac{t_{Dxf}}{\omega}\right)^{1/4} \qquad (2.1)$$

Substituting the dimensionless quantities, *Equations. 1.1, 1.2.c* and *1.3* into *Equation 2.1*, yields:

$$\Delta P_{wf} = \frac{44{,}102 q\mu B}{k_{fb} h\sqrt{C_{fD}}}\left(\frac{k_{fb}}{\phi\mu (c_t)_{f+m} x_f^2 \omega}\right)^{0{,}25} t^{0{,}25} \qquad (2.2.a)$$

For pressure buildup analysis, application of time superposition is required, therefore *Equation 2.2.a* becomes:

$$\Delta P_{ws} = \frac{44{,}102 q\mu B}{k_{fb} h\sqrt{C_{fD}}}\left(\frac{k_{fb}}{\phi\mu (c_t)_{f+m} x_f^2 \omega}\right)^{0{,}25} \left(\sqrt{t_p+\Delta t} - \sqrt{\Delta t}\right) \qquad (2.2.b)$$

The above expressions imply that a Cartesian plot of ΔP vs. either $t^{0,25}$ or $[(t_p+\Delta t)^{0,25} - \Delta t^{0,25}]$ will yield a straight line with slope, m_{BL}:

$$m_{BL} = \frac{44{,}102 q\mu B}{k_{fb} h\sqrt{C_{fD}}}\left(\frac{k_{fb}}{\phi\mu (c_t)_{f+m} x_f^2 \omega}\right)^{0{,}25} \qquad (2.3)$$

Solving for the fracture conductivity, $k_f w_f$, results:

$$k_f w_f = \frac{1944{,}96}{\sqrt{\omega\mu(\phi c_t)_{f+m} k_{fb}}}\left(\frac{q\mu B}{h\, m_{BL}}\right)^2 \qquad (2.4)$$

Figure 1 is a plot of $P_D C_{fD}^{\ 0,5} \lambda_f^{\ 0,25}$ versus $\lambda\, t_{Dxf}/\omega$. It is observed there that during the pseudosteady state transition period $P_D \lambda_f^{\ 0,5}$ yields a horizontal line defined by Tiab and Bettam (2007) as:

$$P_{Dpss} C_{fD}^{\ 0,5} \lambda_f^{\ 0,25} = \frac{\pi}{\sqrt{2}} \qquad (2.5)$$

Replacing *Equations 1.1* and *1.3* into *Equation 2.5* and solving for λ_f yields:

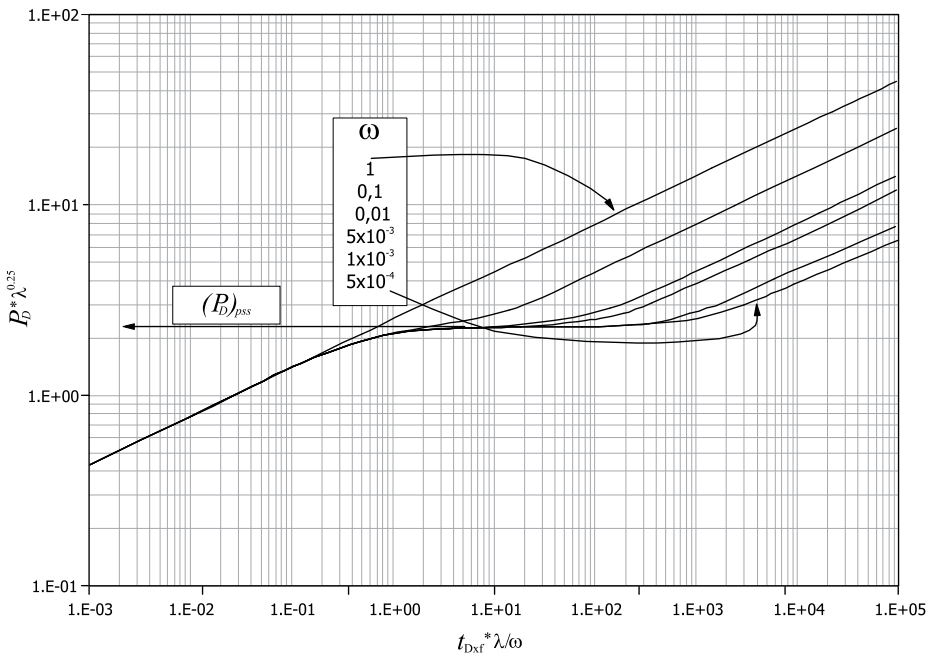

Figure 1. Effect of the dimensionless storativity ratio on the dimensionless pressure behavior for a finite-conductivity fracture, after Tiab and Bettam (2007)

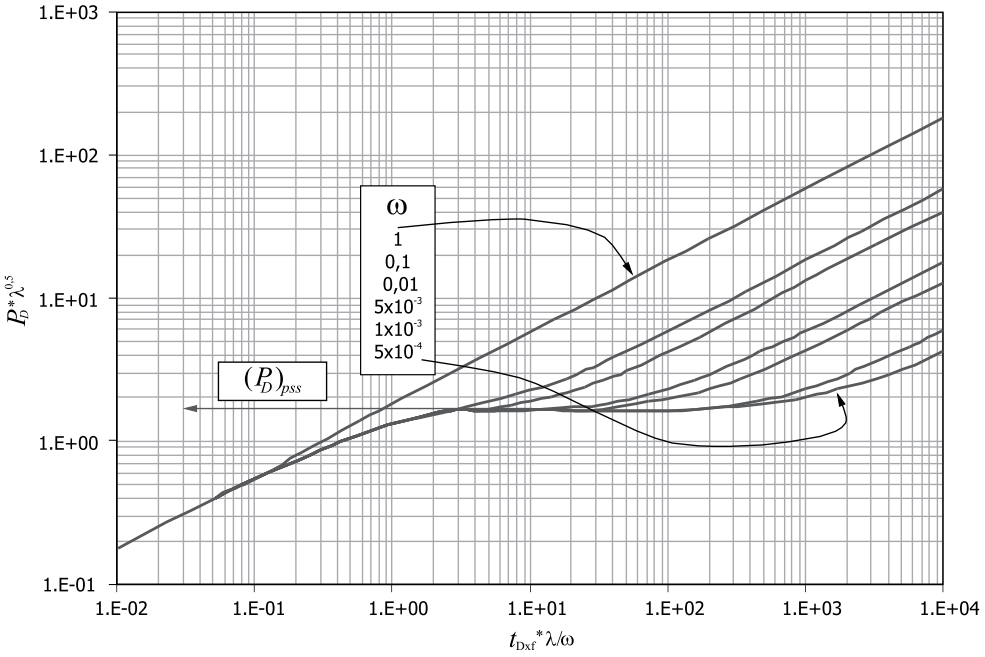

Figure 2. Effect of the dimensionless storativity ratio on the dimensionless pressure behavior for an infinite-conductivity fracture, after Tiab and Bettam (2007)

$$\sqrt{\frac{k_f w_f}{k_{fb} x_f}}\,\lambda_f^{0.25} = 313{,}667\frac{q\mu B}{k_{fb}h(\Delta P)_{pss}} \qquad (2.6)$$

It is observed for the first bilinear flow regime that the curves for the same interporosity flow parameter coincide for different values of dimensionless capacity ratio. See Figure 1. A correlation for this line yields:

$$\omega = 0{,}009745270024\,\frac{\lambda_f k_{fb}}{\phi\mu(c_t)_{f+m}x_f^2}\left(\frac{k_{fb}h\Delta P_{lhr}C_{fD}^{0.5}\lambda_f^{0.25}}{141{,}2\,q\mu B}\right)^{-3{,}96430663} \qquad (2.7)$$

Equation 2.7 has a correlation coefficient of 0,99994583 and should be valid for $\omega \geq 0{,}005$.

Also, according to Tiab and Bettam (2007), the linear flow regime during early time is governed by:

$$P_D = \sqrt{\frac{t_{Dxf}}{\omega}} \qquad (2.8)$$

Substituting in *Equation 2.8* the dimensionless quantities, *Equations 1.1* and *1.2.c*, respectively, yields:

$$\Delta P_{wf} = 4{,}064\left(\frac{qB}{x_f h}\right)\sqrt{\frac{\mu}{\omega(\phi c_t)_{f+m}k_{fb}}}\,t^{0.5} \qquad (2.9.a)$$

Application of time superposition to *Equation* 2.9.a leads to:

$$\Delta P_{ws} = 4{,}064\left(\frac{qB}{x_f h}\right)\sqrt{\frac{\mu}{\omega(\phi c_t)_{f+m}k_{fb}}}\left(\sqrt{t_p+\Delta t}-\sqrt{\Delta t}\right) \qquad (2.9.b)$$

Equations 2.9.a and *2.9.b* imply that a Cartesian plot of ΔP vs. either $t^{0,5}$ or $[(t_p+\Delta t)^{0,5}- \Delta t^{0,5}]$ will yield a straight line with slope, m_L:

$$m_L = 4{,}064\left(\frac{qB}{x_f h}\right)\sqrt{\frac{\mu}{(\phi c_t)_{f+m}k_{fb}\omega}} \qquad (2.10)$$

Solving for the fracture conductivity, x_f, results:

$$x_f = 4{,}064\left(\frac{qB}{m_L h}\right)\sqrt{\frac{\mu}{(\phi c_t)_{f+m}k_{fb}\omega}} \qquad (2.11)$$

Figure 2 is a plot of $P_D\lambda_f^{0,5}$ versus $\lambda_f t_{Dxf}/w$. As pointed out by Tiab and Bettam (2007), it is observed that during

the pseudosteady state transition period $P_D\lambda_f^{0,5}$ is a horizontal line:

$$P_{DPSS}\lambda^{0,5} = \frac{\pi}{2} \qquad (2.12)$$

Substituting for the dimensionless term, *Equation 1.1*, and solving for λ_f results:

$$\lambda_f^{0,5} = 221,8\,\frac{q\mu B}{k_{fb}h\,(\Delta P)_{pss}} \qquad (2.13)$$

Notice that for the first linear flow, the lines for the same interporosity flow parameter coincide for different values of storativity coefficient ratio. A correlation for this line yields:

$$\omega = 0,0008369600544\,\frac{\lambda_f k_{fb}}{\phi\mu(c_t)_{f+m}x_f^2}\left(\frac{k_{fb}h\Delta P_{lhr}\lambda_f^{0,5}}{141,2\,q\mu B}\right)^{-1,984944590} \qquad (2.14)$$

Equation 2.14 has a correlation coefficient of 0,999971228 and should be valid for $\omega \geq 0,005$.

Finally, Tiab and Bettam (2007) found that the pressure derivative displays a maximum pressure once the transition period begins, and a minimum point during the transition period. If these points are feasible of being obtained, the dimensionless storativity ratio can be estimated for bilinear and linear flow regime, respectively, by:

$$\omega = \exp\left(-0,229\,\frac{t_{min}}{t_{max}}\right) \qquad (2.15)$$

$$\omega \approx \frac{k_{fb}t_{max}}{1896,1\lambda\mu(\phi c_t)_{f+m}x_f^2} \qquad (2.16)$$

THE TRANSITION PERIOD OCCURS AFTER RADIAL FLOW REGIME

In elongated reservoirs where the mass transfer between matrix and fractures is delayed due to very low interporosity flow parameters, less than $1x10^{-7}$, the transition period takes places once radial flow regime has vanished. Either dual-linear or single-linear flow regime may be interrupted by the transition period in which the fracture network is fed by the matrix. For the case of transient rate analysis, this behavior may show up during the late pseudosteady state period, though.

Figure 3 displays a semilog plot of the dimensionless pressure, times the square-root of the interporosity flow parameter versus dimensionless time for different dimensionless capacity ratios. This plot can provide better detail than the pure dimensionless pressure plots. As expected, an early linear trend is observed indicating the infinite transient behavior. Afterwards, the dual- linear flow regime appears. However, part of it is obscured by the radial flow regime. During the late pseudosteady state period, all the lines for different dimensionless storativity ratios coincide for each interporosity flow parameter.

Figure 4 is a semilog plot of the dimensionless pressure versus dimensionless time for different values of the interporosity flow parameter and storativity coefficient ratios. Part of the transition period is shown in the plot. It is observed that the lines for the same storativity coefficient ratio coincide for the same value of the interporosity flow parameter. A correlation between ω and the intercept of the semilog plot has a correlation coefficient of 0,99999872 and a standard deviation of $3,2973259x10^{-5}$. The range of application of this correlation is $0,01 \leq \omega \leq 0,1$ and $-5 \leq s_r \leq 5$. This is given below as:

$$\omega = \text{anti log}\left[-3,224536 + 1,000046077\log\left(\frac{k_{fb}}{\mu\phi(c_t)_{f+m}r_w^2}\right) - \frac{k_{fb}h\Delta P_{lhr}}{162,44697q\mu B} - S_r\right] \qquad (3.1)$$

As shown in Figure 5, the intercept of the semilog plot is a direct function of the skin factor. The correlation between skin factor and the intercept is shown in Figure 6. *Equation 3.1* already includes this effect.

The interporosity flow parameter can be approximated by the equation provided by Tiab and Escobar (2003):

$$\lambda = \frac{3792(\phi c_t)_i\mu r_w^2}{k_{fb}\Delta t_{inf}}\left[\omega\ln\left(\frac{1}{\omega}\right)\right] \qquad (3.2)$$

The Transition Period Occurs During The Dual-Linear Flow Regime

Escobar *et al.* (2009) presented the governing equation for dual-linear flow regime in a naturally fractured reservoir:

$$P_D = \frac{2\sqrt{\pi t_D}}{W_D\sqrt{\omega}} + S_{DL} \qquad (3.3)$$

After replacing the dimensionless quantities in the above expression, it yields:

$$\Delta P_{wf} = \frac{8{,}1282}{Y_E}\frac{qB}{h}\left(\frac{\mu}{\phi c_t k_{fb}\omega}\right)^{0,5}\sqrt{t} + \frac{141{,}2\,q\mu B}{k_f h}S_{DL} \qquad (3.4)$$

For pressure buildup analysis, application of time superposition is required, therefore *Equation 3.4* becomes:

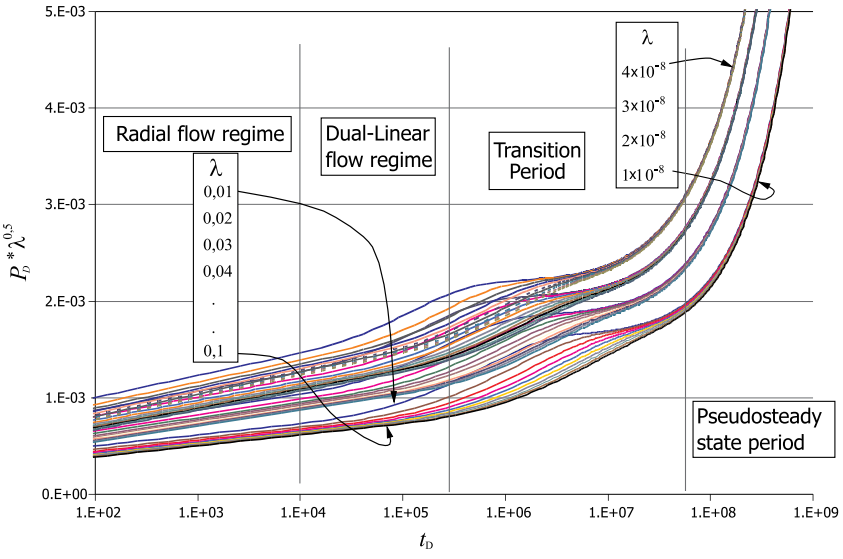

Figure 3. Semilog plot of dimensionless pressure times the square-root of the interporosity flow parameter versus dimensionless time for different dimensionless storativity ratios without wellbore storage – Well centered in the reservoir

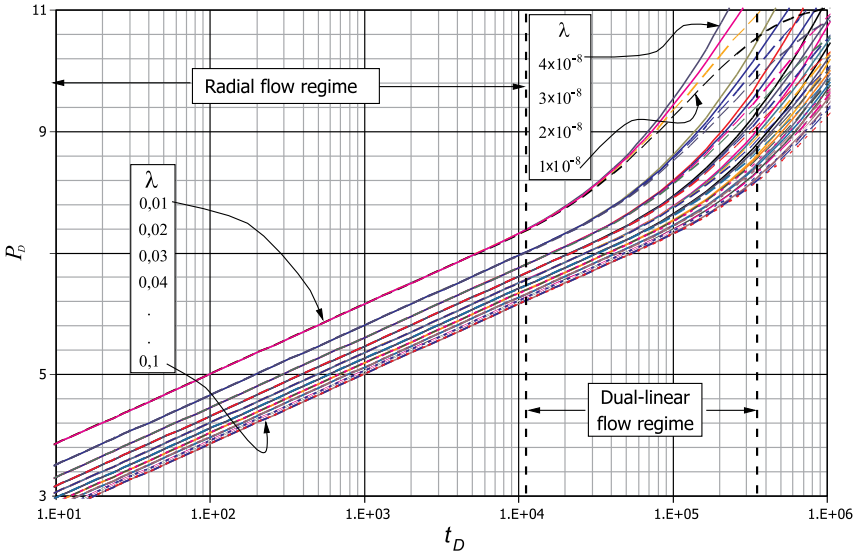

Figure 4. Semilog plot of dimensionless pressure versus dimensionless time for different values of the interporosity flow parameter and storativity coefficient ratios - Well centered in the reservoir

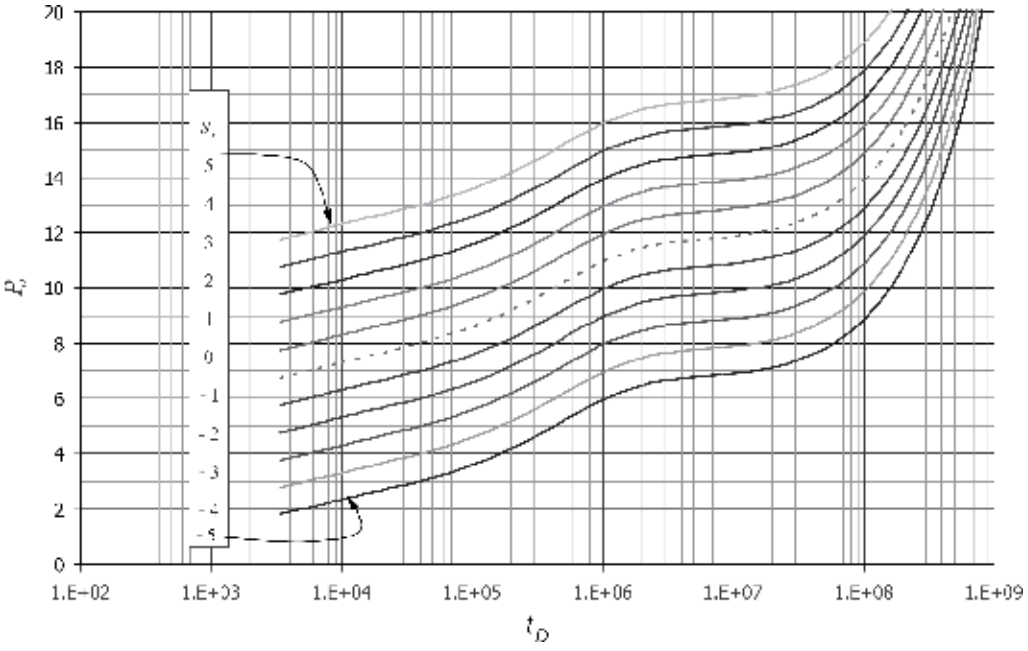

Figure 5. Semilog plot of dimensionless pressure versus dimensionless time for ω = 0,01 and λ = 1x10^{-8} with different mechanical skin factors - Well centered in the reservoir

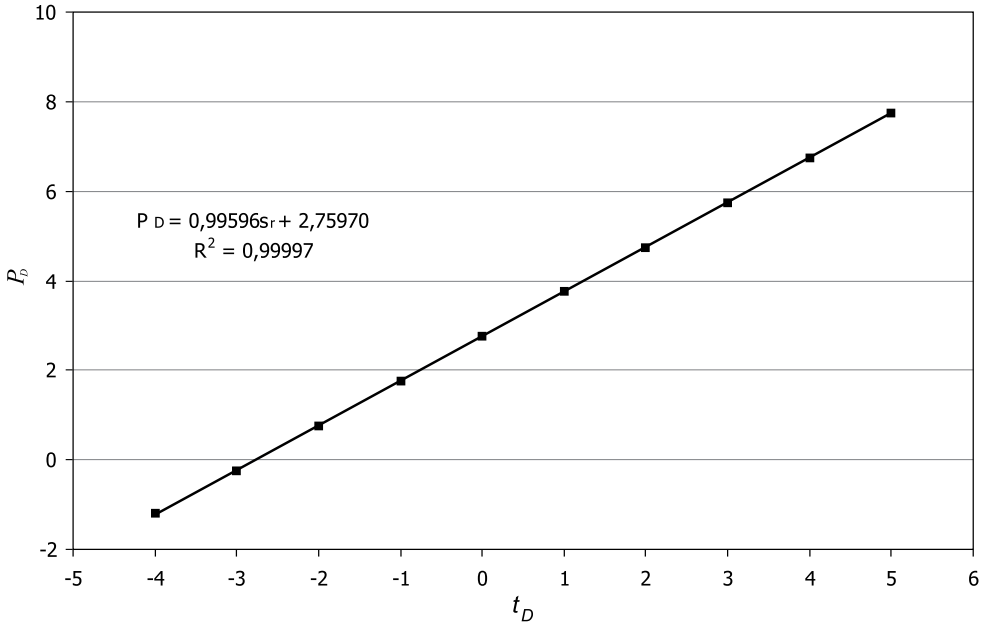

Figure 6. Relationship between the dimensionless pressure with the mechanical skin factors, for ω = 0,01 and λ = 1x10^{-8} - Well centered in the reservoir

$$\Delta P_{ws} = \frac{8,1282}{Y_E}\frac{qB}{h}\left(\frac{\mu}{\phi c_t k_{fb}\omega}\right)^{0,5}\left(\sqrt{t_p+\Delta t}-\sqrt{\Delta t}\right) \qquad (3.5)$$

Equations 3.4 and *3.5* indicate that a Cartesian plot of ΔP vs. either $t^{0,5}$ or $[(t_p+\Delta t)^{0,5}- \Delta t^{0,5}]$ will yield a straight line during dual-linear flow behavior which slope, m_{DLF}, and intercept, b_{DLF}, are used to obtain reservoir width, Y_E, once the storativity coefficient ratio is determined and dual-linear skin factor, s_{DL}.

$$Y_E = \frac{8,1282}{m_{DLF}h}\left[\frac{\mu}{k_{fb}\phi c_t\omega}\right]^{0,5} \qquad (3.6)$$

$$S_{DL} = \frac{k_{fb}h\,b_{DLF}}{141,2q\mu B} \qquad (3.7)$$

Linear-Flow Regime Occurs After The Transition Period

Once the transition period disappears, the reservoir behaves as homogeneous; then, the single-linear flow regime appears, which governing equations for pressure and pressure derivative presented by Escobar *et al.* (2007a) and Escobar and Montealegre (2007) are:

$$P_D = \frac{2\pi\sqrt{t_D}}{W_D} + S_L \qquad (3.8)$$

Replacing *Equations 1.1, 1.2.a* and *1.4* into the above expression results:

$$\Delta P_{wf} = \frac{14,407}{Y_E}\frac{qB}{h}\left(\frac{\mu}{\phi c_t k_{fb}}\right)^{0,5}\sqrt{t} + \frac{141,2\,q\mu B}{k_f h}S_L \qquad (3.9)$$

and for buildup pressure tests *Equation 3.9* becomes:

$$\Delta P_{ws} = \frac{14,407}{Y_E}\frac{qB}{h}\left(\frac{\mu}{\phi c_t k_{fb}}\right)^{0,5}\left(\sqrt{t_p+\Delta t}-\sqrt{\Delta t}\right) \qquad (3.10)$$

This implies that a Cartesian plot of ΔP vs. either $t^{0,5}$ or $[(t_p+\Delta t)^{0,5}- \Delta t^{0,5}]$ will yield a straight line during dual-linear flow behavior which slope, m_{LF}, and intercept, b_{LF}, are used to obtain reservoir width, Y_E, once the storativity coefficient ratio is determined and linear skin factor, S_L.

$$Y_E = \frac{14,407}{m_{LF}h}\left[\frac{\mu}{k_{fb}\phi c_t}\right]^{0,5} \qquad (3.11)$$

$$S_L = \frac{k_{fb}h\,b_{DLF}}{141,2q\mu B} \qquad (3.12)$$

Linear-Flow Regime Occurs Before The Transition Period

According to Escobar *et al.* (2009), this case, which is described by Figures 7 and 8, has the following governing equation:

$$P_D = \frac{10\pi\sqrt{t_D}}{6W_D\sqrt{\omega}} + S_L \qquad (3.13)$$

Once the dimensionless quantities are replaced in *Equation 3.13*, the following expression is obtained:

$$\Delta P_{wf} = \frac{12,006}{Y_E}\frac{qB}{h}\left(\frac{\mu}{\phi c_t k_{fb}\omega}\right)^{0,5}\sqrt{t} + \frac{141,2\,q\mu B}{k_{fb}h}S_L \qquad (3.14)$$

For pressure buildup analysis, application of time superposition is required, therefore *Equation 3.14* becomes:

$$\Delta P_{wf} = \frac{12,006}{Y_E}\frac{qB}{h}\left(\frac{\mu}{\phi c_t k_{fb}\omega}\right)^{0,5}\left(\sqrt{t_p+\Delta t}-\sqrt{\Delta t}\right) \qquad (3.15)$$

This implies that a Cartesian plot of ΔP vs. either $t^{0,5}$ or $[(t_p+\Delta t)^{0,5}- \Delta t^{0,5}]$ will yield a straight line during linear flow behavior which slope, m_{LF}, and intercept, b_{LF}, are used to obtain reservoir width, Y_E, once the storativity coefficient ratio is determined and single-linear skin factor, S_L.

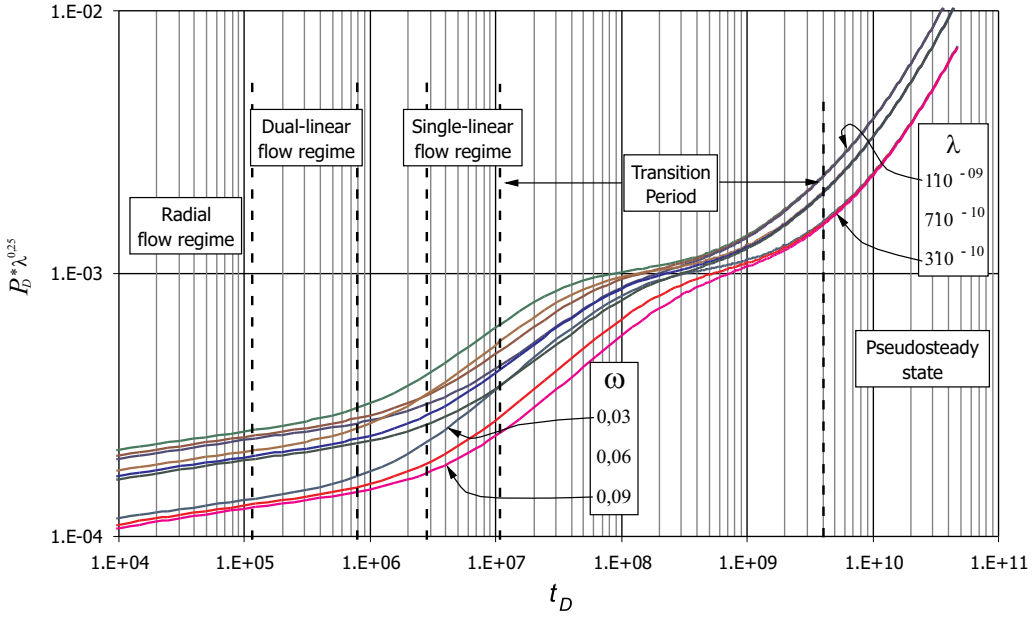

Figure 7. Log-log plot of dimensionless pressure times the square-root of the interporosity flow parameter versus dimensionless time for different values of interporosity flow parameter and storativity ratios - Well off-centered in the reservoir

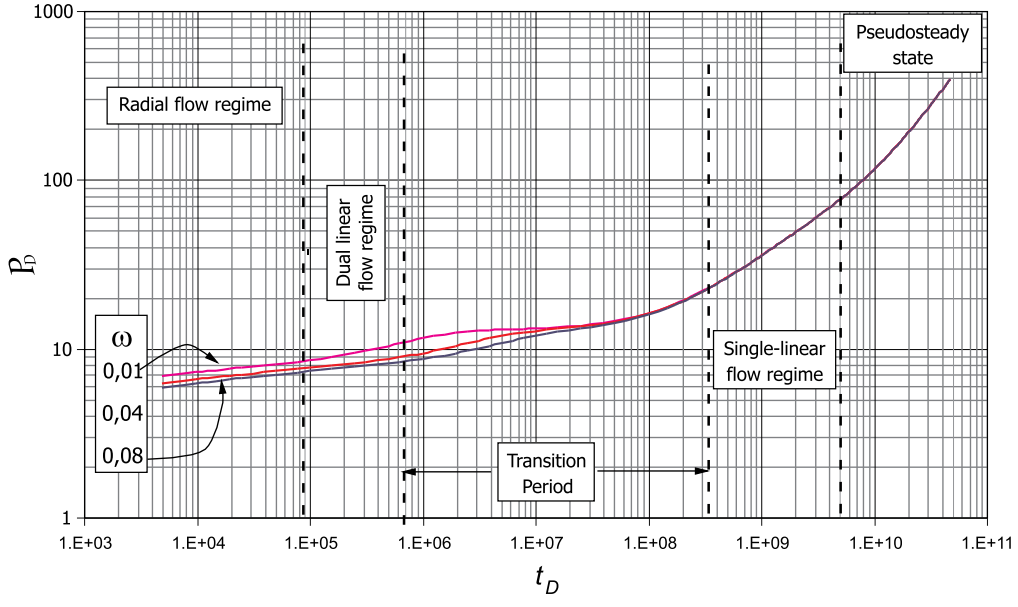

Figure 8. Log-log plot of dimensionless pressure versus dimensionless time for different values of the dimensionless storativity ratio and $\lambda = 1 \times 10^{-8}$, presence of homogeneous single-linear flow – Well off-centered in the reservoir

EXAMPLES

Synthetic Example 1

A synthetic pressure test for a well in an infinite reservoir was generated by Tiab and Bettam (2007) with information from Table 1. Characterize this hypothetic reservoir using conventional analysis.

Solution

In this example the bilinear flow regime occurs before the transition period. From Figure 9, we read a value of $\Delta P_{1hr} = 101{,}5$ psi, $t_{min} = 0{,}095$ hr, $t_{max} = 0{,}0073$ hr, and $\Delta P_{pss} = 37{,}5$ psi. Values of $m_{BL} = 96{,}96$ psi/hr are read from Figure 10. The calculations are summarized below:

Table 1. Summary of results for synthetic example 1

	Tiab and Bettam (2007)	This study – Eq.
Parameter	Value	
λ_f	4,2	4,15 - 2,6
λ	$5x10^{-6}$	$4{,}86x10^{-6}$ - 3,2
ω	0,05	0,0634 - 2,7
ω	0,05	0,0508 - 2,15
$k_f w_f$	8227,1 mD-ft	8319,9 mD-ft - 2,4

Synthetic Example 2

A simulated pressure test for a well in an infinite reservoir was generated for this work with information from Table 1. Use conventional analysis to interpret this well pressure test.

Solution

In this example the linear flow regime occurs before the transition period. From Figure 11, we read a value of $\Delta P_{1hr} = 492{,}0$ psi, $t_{max} = 0{,}0072$ hr and $\Delta P_{pss} = 82{,}0$ psi. Values of $m_L = 730{,}9$ psi/hr are read from Figure 12. A summary of results is given below:

Table 2. Summary of results for synthetic example 2

Parameter	Simulation	Value
λ_f		1,08 - 2,13
λ	$1x10^{-6}$	$1{,}05x10^{-6}$ - 3,2
ω	0,01	0,041 - 2,14
ω	0,01	0,013 - 2,16
x_f	200	234 - 2,11

Synthetic Example 3

The semilog plot of a simulated drawdown generated with the information of Table 1, presented by Escobar *et al.* (2009) is reported in Figure 13. Characterize this hypothetic reservoir using conventional analysis.

Solution

From Figure 13, $\Delta P1hr = 378{,}81$ psi is read. Values of $m_{DLF} = 36{,}36$ psi/hr and $b_{DLF} = 346{,}36$ psi are read from Figure 14. The computations are summarized and reported as follows:

Table 3. Summary of results for synthetic example 3

	Simulation Input	Escobar *et al.* (2009)	This study - Eq.
Parameter	Value		
ω	0,08	0,0841	0,0812 - 3,1
λ	$1x10^{-8}$	$2{,}295x10^{-8}$	$8{,}56x10^{-9}$ - 3,2
Y_E,ft	1800	1794,21	1890,3 - 3,6
^{S}DL		6,74	6,76 - 3,7

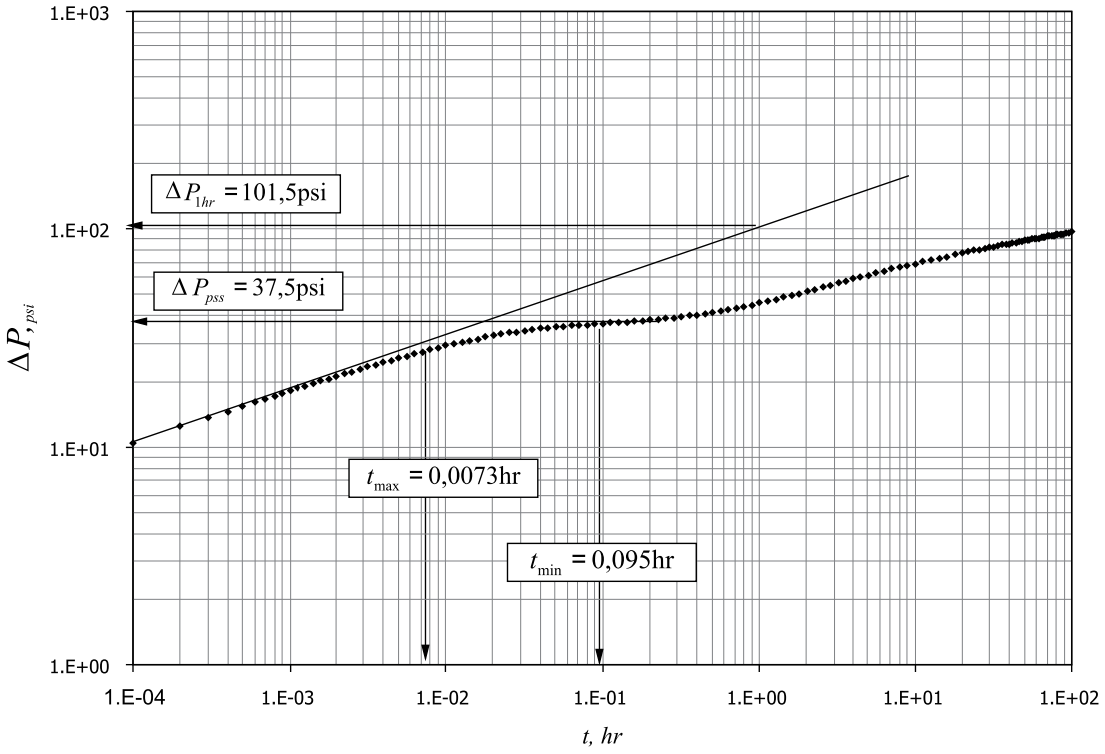

Figure 9. Log-log plot of pressure drop vs. *t* for synthetic example 1

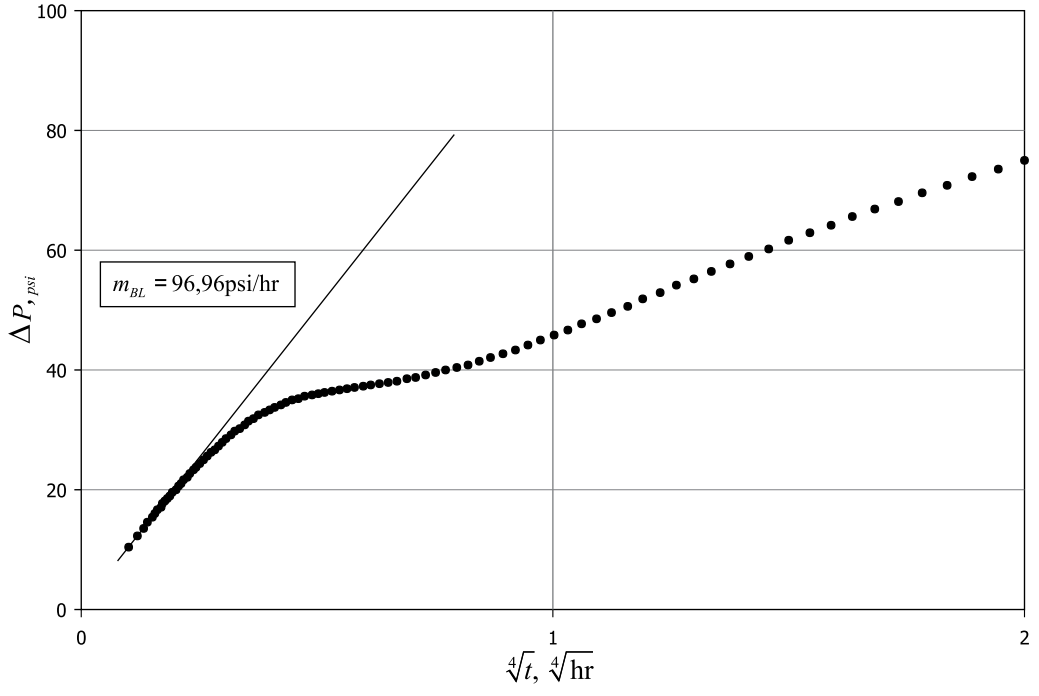

Figure 10. Cartesian plot of pressure drop vs. $t^{0,25}$ for synthetic example 1

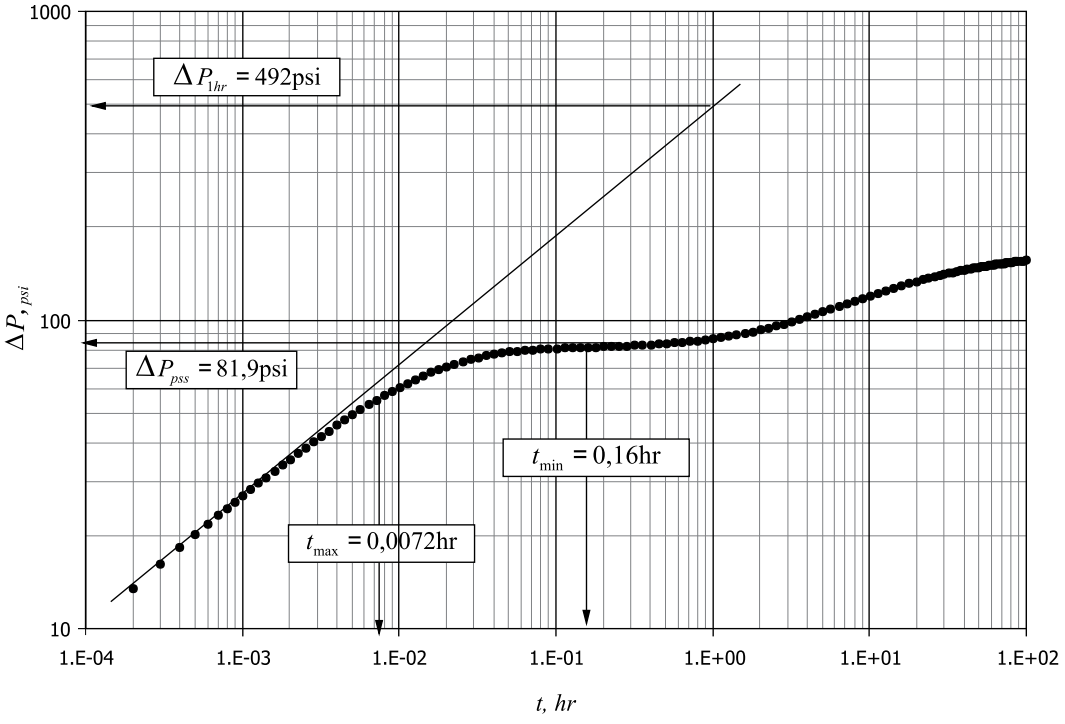

Figure 11. Log-Log plot of pressure drop vs. *t* for synthetic example 2

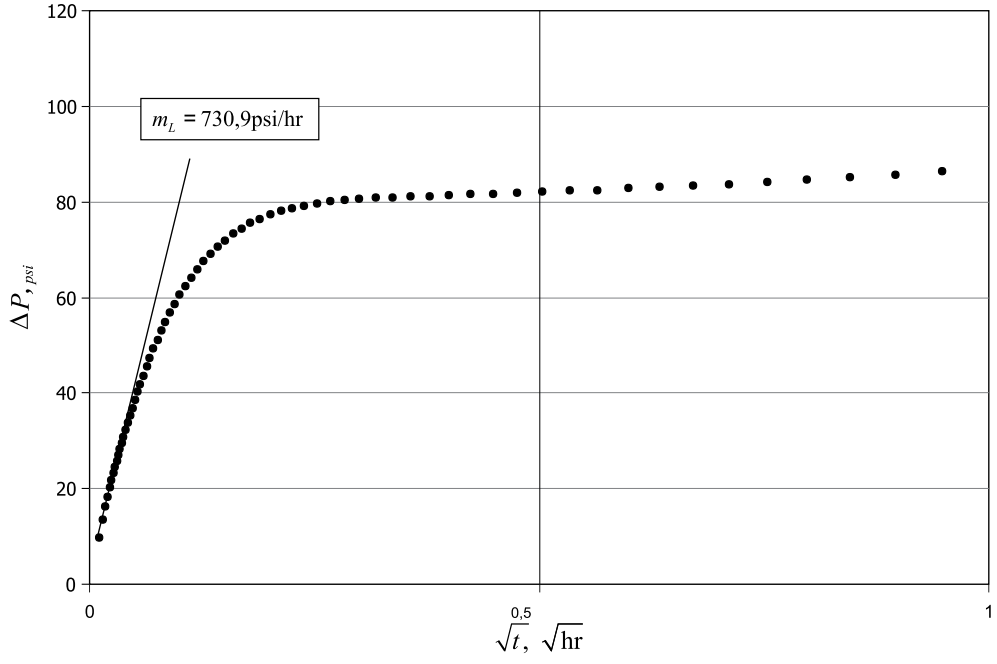

Figure 12. Cartesian plot of pressure drop vs. $t^{0,5}$ for synthetic example 2

Synthetic Example 4

A synthetic pressure test for a well off-centered in a reservoir was also generated by Escobar *et al.* (2009) with information from Table 1. The pressure and pressure derivative plot is provided in Figure 15. It is required to estimate the geometric skin factors, reservoir width and the naturally fractured reservoir parameters.

Solution

From Figure 15, it is read a value of $\Delta P1\text{hr} = 409{,}703$ psi. Values of $m_{DLF} = 133{,}68$ psi/hr, $b_{DLF} = 314{,}81$, $m_{LF} = 201{,}55$ psi/hr and $b_{LF} = 211{,}77$ psi are read from Figure 16. The computations are summarized and reported as follows:

Table 4. Summary of results for synthetic example 4

	Simulation Input	Escobar *et al.* (2009)	This study - Eq.
Parameter	Value		
ω	0,03	0,029	0,0109 - 3,1
λ	$1\text{x}10^{-9}$	$3{,}14\text{x}10^{-8}$	$4{,}42\text{x}10^{-9}$ - 3,2
Y_E,ft	1500	1511,5	1510,5 - 3,6
Y_E,ft	1500	1513,1	1497,98 - 3,11
^{S}DL	8,6	2,12	6,69 - 3,7

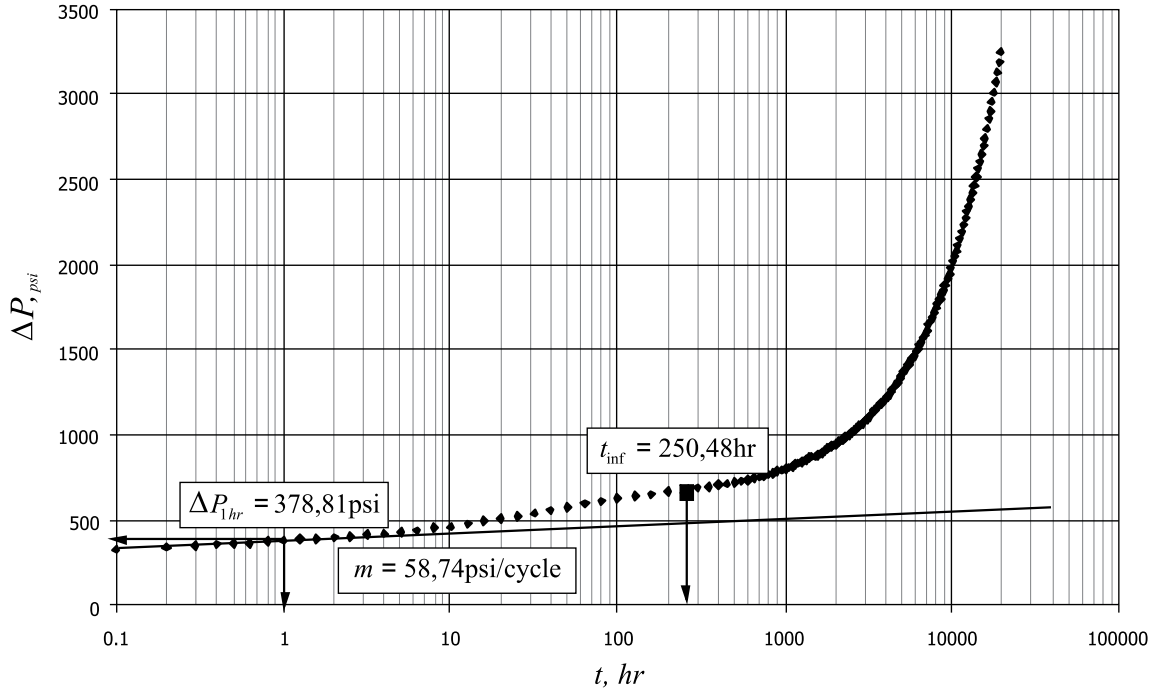

Figure 13. Semilog plot of pressure drop vs. time for synthetic example 3

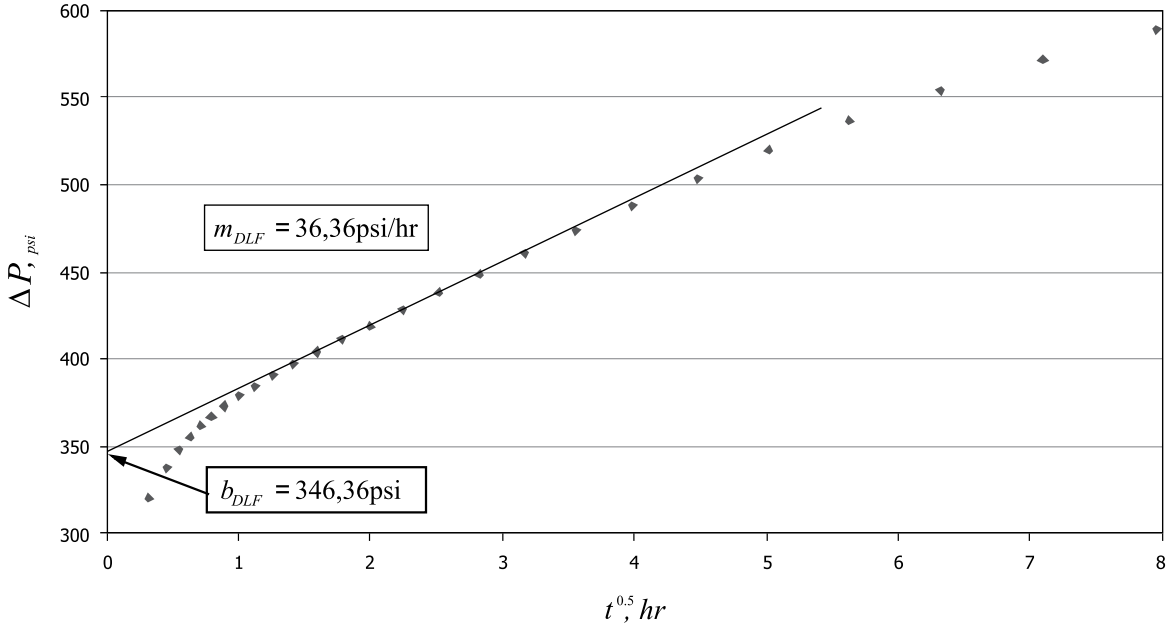

Figure 14. Cartesian plot of pressure drop vs. $t^{0.5}$ for synthetic example 3

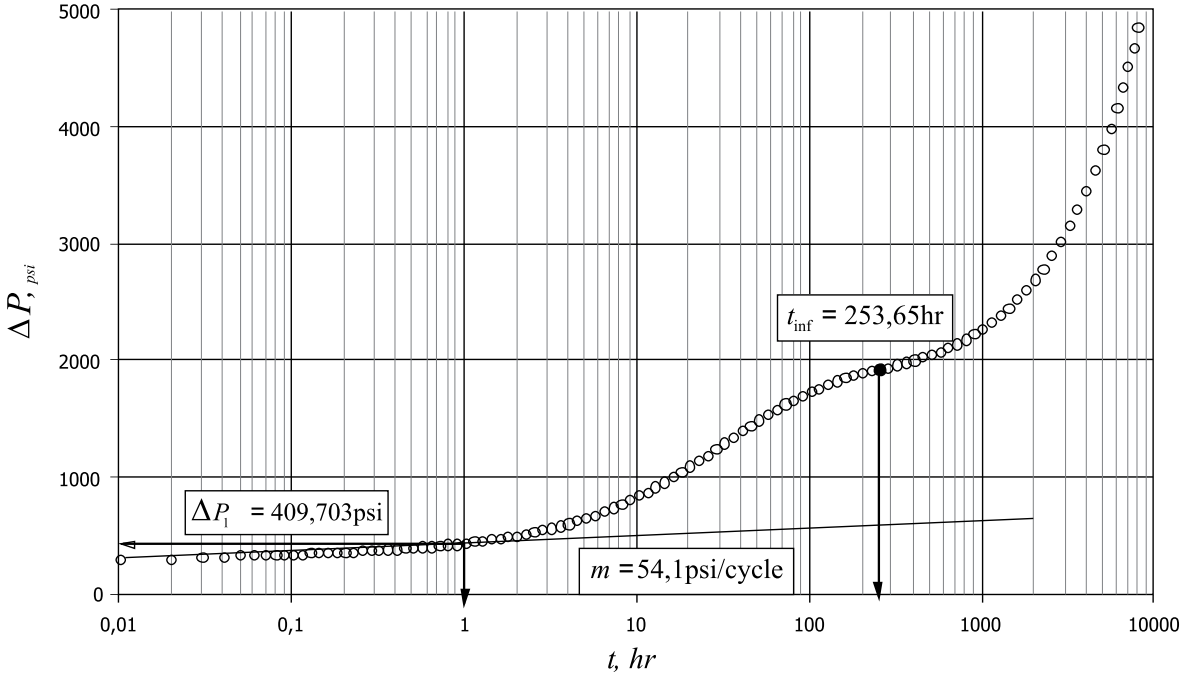

Figure 15. Semilog plot of pressure drop vs. time for synthetic example 4

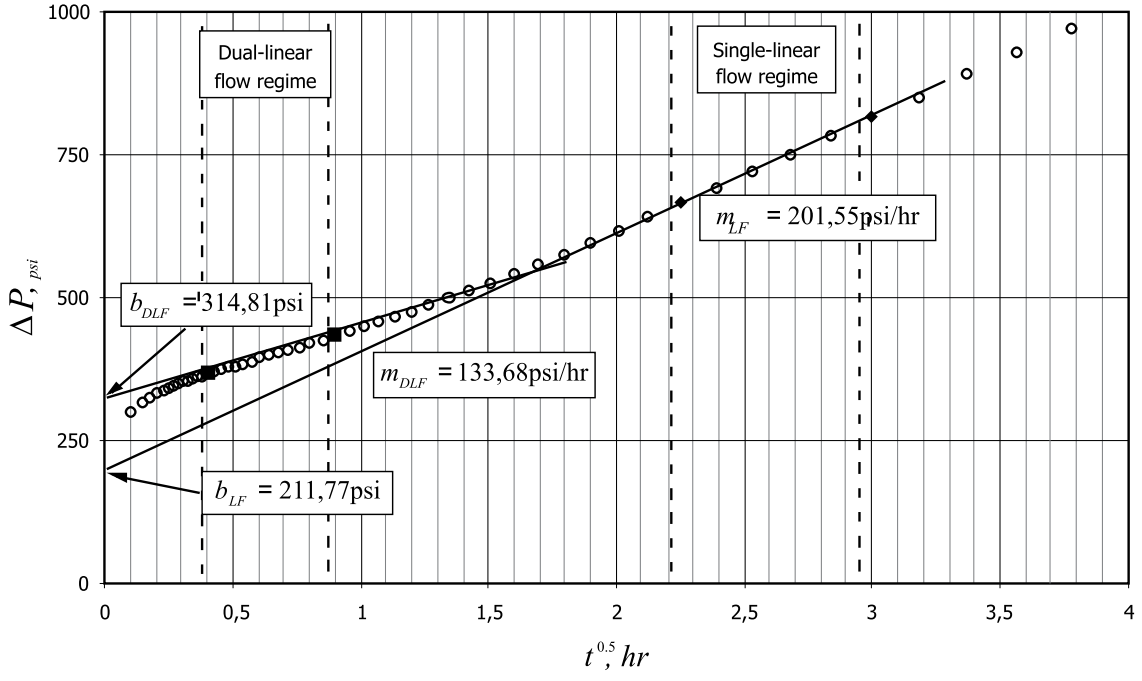

Figure 16. Cartesian plot of pressure drop vs. $t^{0,5}$ for synthetic example 4

Field Example

Escobar *et al.* (2009) also reported an example taken from a pressure test run in a South American well. Reservoir, fluid and well parameters are provided in Table 1 and the pressure data is provided in Figure 17. The reservoir permeability of 2700 md was obtained from a previous test. Find reservoir width, geometric skin factor, interporosity flow parameter and the dimensionless storativity coefficient.

Solution

In this example the single-linear flow regime occurs after the transition period. Since permeability is known, the semilog slope can be found from the classical conventional equation giving a value of 4,58 psi/cycle. Then, $\Delta P_{1hr} = 21,16$ psi is obtained using any point on the radial flow regime straight line from Figure 17. Values of $m_{DLF} = 35,87$ psi/hr, $b_{DLF} = 8,47$, $m_{LF} = 18,55$ psi/hr and $b_{LF} = 13,53$ psi are read from Figure 18. The computations are summarized and reported as follows:

Table 5. Summary of results for synthetic example 5

	Escobar *et al.* (2009)	This study – Eq.
Parameter	Value	
ω	0,074	0,035 - 3,1
λ	$3,14x10^{-8}$	$1,4x10^{-6}$ - 3,2
Y_E,ft	446,4	679,65 - 3,6
Y_E,ft	446,4	435,92 - 3,16
s_{DL}	12,2	6,69 - 3,7
s_L	4,32	6,76 - 3,17

COMMENTS ON THE RESULTS

The synthetic examples are shown to verify the introduced equations for the conventional technique. A good agreement is observed between the results obtained in this study and those from the simulation input or other sources. However, the results of the field example showed disagreement to some extent, probably due to the noisy data, as well as the accuracy of the correlations.

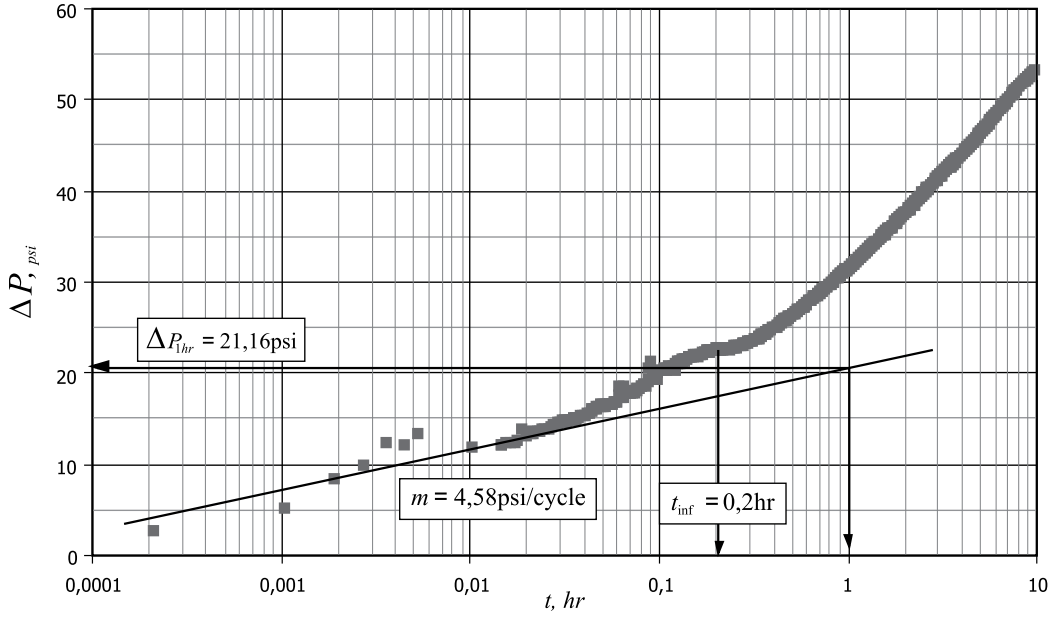

Figure 17. Semilog plot of pressure drop vs. time for the field example

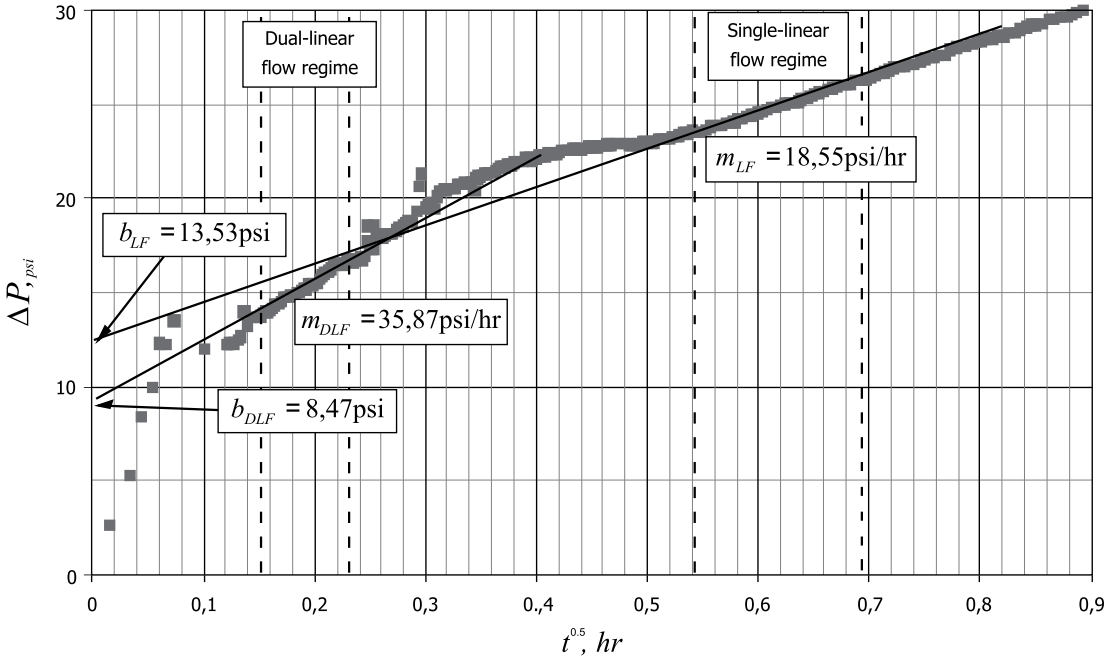

Figure 18. Cartesian plot of pressure drop vs. $t^{0.5}$ for the field example

Table 6. Data used for the simulation runs and examples

	Example 1	Example 2	Simulation runs	Example 3	Example 4	Field case
Parameter	Value					
q,BPD	1000	2000	300	300	500	457
k_{fb}, md	40	100	33,34	25	50	2700
s			0	0		
h, ft	100	50	30	50	30	84
c_t	4×10^{-6}	4×10^{-6}	3×10^{-6}	3×10^{-6}	3×10^{-6}	$9{,}899 \times 10^{-6}$
r_w, ft	0,25	0,35	0,3	0,35	0,5	0,5
ϕ, %	0,2	0,2	10	15	10	7,34
P_i,psi	3000	4000	5000	5000	4000	
B, rb/STB	1,05	1,2	1	1,2	1	1,49
Y_E,ft			1000	1800	1500	
x_f ft	200	200				
μ, cp	0,65	0,8	1	1,26	1	9,4
A,ft^2			20×10^6	$28{,}8 \times 10^6$	$40{,}5 \times 10^6$	
λ	5×10^{-6}	1×10^{-6}		1×10^{-8}	1×10^{-9}	
λ_f	3,2	1				
ω	0,05	0,01		0,08	0,03	

CONCLUSION

- New equations for the classical conventional method are introduced to characterize oil bearing heterogeneous formation when the transition period takes place outside the radial flow regime. The equation provided by Tiab and Escobar (2003) to determine the interporosity flow parameter, initially developed for transition period during the radial flow regime, has been found to provide good results for heterogeneous formations when the transition period takes place before or after the radial flow regime.

ACKNOWLEDGMENTS

The authors gratefully acknowledge the financial support of Universidad Surcolombiana for the completion of this study.

REFERENCES

Escobar, F. H., Hernandez, D. P. & Saavedra, J. A. (2009). Pressure and pressure derivative analysis for long naturally fractured reservoirs using the tds technique. *Article sent to the Dyna Journal to request publication.*

Escobar, F. H., Hernández, Y. A. & Hernández, C. M. (2007) a. Pressure transient analysis for long homogeneous reservoirs using tds technique. *J. of Petroleum Science and Engineering,* 58 (1-2), 68-82.

Escobar, F. H. & Montealegre, M. (2007). A complementary conventional analysis for channelized reservoirs. *CT&F- Ciencia, Tecnología y Futuro*. 3(3), 137-146.

Escobar, F. H., Tiab, D. & Tovar, L.V. (2007). Determination of areal anisotropy from a single vertical pressure test and geological data in elongated reservoirs. *J. of Engineering and Applied Sciences*, 2(11), 1627-1639.

Tiab, D. & Escobar, F. H. (2003). Determinación del parámetro de flujo interporoso a partir de un gráfico semilogarítmico. *X Congreso Colombiano del Petróleo* (Colombian Petroleum Symposium). Bogotá, Colombia.

Tiab, D. & Bettam, Y. (2007). Practical interpretation of pressure tests of hydraulically fractured wells in a naturally fractured reservoir. *Paper SPE 107013 presented at the SPE Latin American and Caribbean Petreoleum Engineering Conference* held in Buenos Aires, Argentina.

Warren, J. E. & Root, P. J. (1963). The behavior of naturally fractured reservoirs. *Soc. Pet. Eng. Journal*, September edition, 245-255.